Stem Cell Research 42 (2020) 101658

Contents lists available at ScienceDirect

Stem Cell Research

journal homepage: www.elsevier.com/locate/scr

Lab resource: Stem Cell Line

Generation of the human induced pluripotent stem cell (hiPSC) line PSMi006-A from a patient affected by an autosomal recessive form of long QT syndrome type 1

Manuela Mura[a], Francesca Bastaroli[b], Marzia Corli[b], Monia Ginevrino[c,d], Federica Calabrò[a], Marina Boni[e], Lia Crotti[f,g,h], Enza Maria Valente[c,d], Peter J. Schwartz[f], Massimiliano Gnecchi[a,b,i,*]

[a] Coronary Care Unit and Laboratory of Experimental Cardiology for Cell and Molecular Therapy, Fondazione IRCCS Policlinico San Matteo, Pavia, Italy
[b] Department of Molecular Medicine, Unit of Cardiology, Università degli studi di Pavia, Pavia, Italy
[c] Department of Molecular Medicine, Unit of Genetics, Università degli studi di Pavia, Pavia, Italy
[d] Neurogenetics Unit, Fondazione IRCCS Santa Lucia, Rome, Italy
[e] Laboratory of Oncohaematological Cytogenetic and Molecular Diagnostics, Division of Haematology, Fondazione IRCCS Policlinico San Matteo, Pavia, Italy
[f] Istituto Auxologico Italiano, IRCCS, Center for Cardiac Arrhythmias of Genetic Origin and Laboratory of Cardiovascular Genetics, Milan, Italy
[g] Istituto Auxologico Italiano, IRCCS, Department of Cardiovascular, Neural and Metabolic Sciences, San Luca Hospital, Milan, Italy
[h] Department of Medicine and Surgery, Università Milano-Bicocca, Milan, Italy
[i] Department of Medicine, University of Cape Town, Cape Town, South Africa

ARTICLE INFO

Keywords:
Endoderm
Mesoderm
Ectoderm

ABSTRACT

We generated human induced pluripotent stem cells (hiPSCs) from dermal fibroblasts of a 40 years old female patient homozygous for the mutation c.535 *G* > *A* p.G179S on the KCNQ1 gene, causing a severe form of autosomal recessive Long QT Syndrome type 1 (AR-LQT1). The hiPSCs, generated using classical approach of the four retroviruses enconding the reprogramming factors OCT4, SOX2, cMYC and KLF4, display pluripotent stem cell characteristics, and differentiate into cell lineages of all three germ layers: endoderm, mesoderm and ectoderm.

Resource Table

Unique stem cell line identifier	PSMi006-A
Alternative name of stem cell line	HDF39-ARLQT-iPS
Institution	Fondazione IRCCS Policlinico San Matteo, Pavia, Italy
Contact information of distributor	Massimiliano Gnecchi, m.gnecchi@unipv.it
Type of cell line	hiPSC
Origin	human
Additional origin info	Age: 40 Gender: female Ethnicity: Caucasian
Cell source	Dermal fibroblasts
Clonality	Clonal
Method of reprogramming	Retroviruses encoding for the human cDNA of OCT4, SOX2, cMYC, KLF4
Genetic modification	No
Type of modification	None
Associated disease	Long QT Syndrome type 1 (OMIM #192,500)
Gene/locus	c.535 *G* > *A* mutation on KCNQ1, chromosomal locus 11p15.5-p15.4, (NM_000218.2)
Method of modification	N/A
Name of transgene or resistance	N/A
Inducible/Constitutive system	N/A
Date archived/stock date	March 15, 2014
Cell line repository/bank	https://hpscreg.eu/cell-line/PSMi006-A
Ethical approval	The study has been approved by the Ethics Committee of our Institution, Fondazione IRCCS Policlinico San Matteo, on the 29th of October 2010, protocol number 20,100,004,354, proceeding P-20,100,003,369. We obtained patient written informed consent for both skin biopsy procedure and conservation of biological samples.

1. Resource utility

It is now well accepted that the iPSC technology can be efficiently

* Corresponding author at: University of Pavia and Fondazione IRCCS Policlinico S. Matteo, Pavia, Italy.
E-mail address: m.gnecchi@unipv.it (M. Gnecchi).

https://doi.org/10.1016/j.scr.2019.101658
Received 29 January 2019; Received in revised form 7 November 2019; Accepted 13 November 2019
Available online 20 November 2019

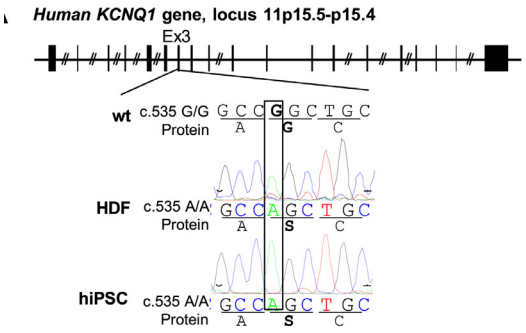

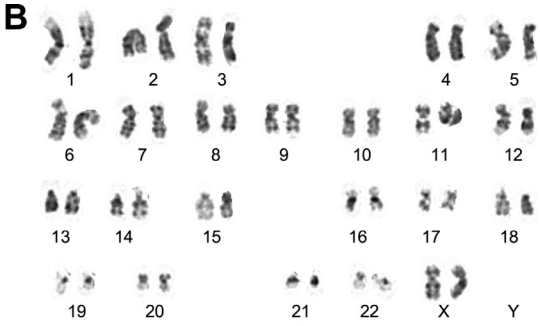

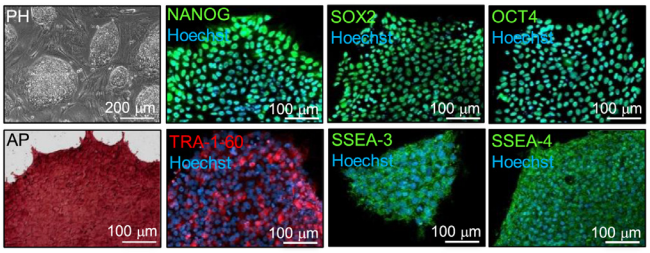

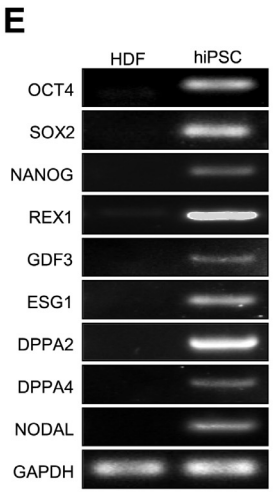

	N° nuclei	N° NANOG⁺ cells	%
Field 1	236	236	100
Field 2	315	306	97,1
Field 3	245	232	94,7
Field 4	248	248	100
TOT	1044	1022	**97,9**

	N° nuclei	N° TRA-1-60⁺ Cells	%
Field 1	420	375	89,7
Field 2	432	398	92,1
Field 3	326	300	92
TOT	1178	1073	**91**

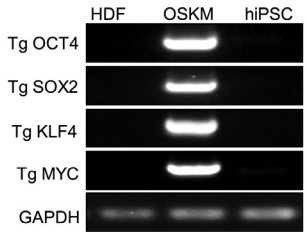

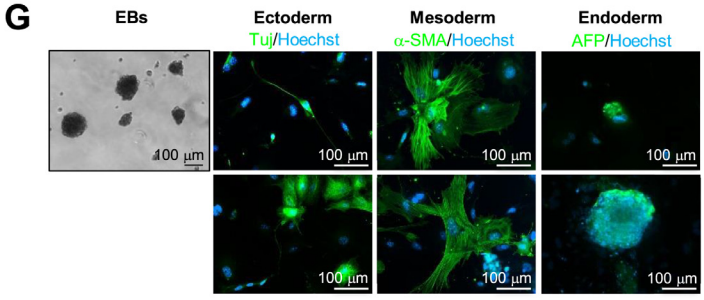

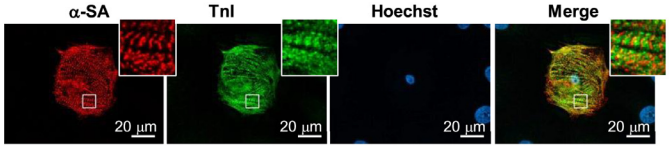

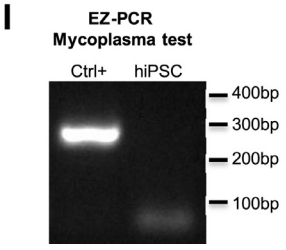

(caption on next page)

used to model LQTS and test targeted therapies (Mehta et al., 2018; Gnecchi et al., 2017; Mura et al., 2017). Accordingly, PSMi006-A will be useful for modeling LQTS type 1 and to test novel targeted drug or molecular approaches.

2. Resource details

PSMi006-A line was generated by reprogramming dermal fibroblasts of 40 years old woman affected by an autosomal recessive form of Long QT Syndrome (LQTS) type 1 (AR-LQT1). LQTS is an inherited

Fig. 1. Characterization of the PSMi006-A cell line. A. On top schematic representation of the *KCNQ1* gene with introns (horizontal lines) and exons (vertical lines/boxes). Bottom, DNA sequencing results showing the presence of the mutation 535 G>A in homozygosis on the Exon 3 of *KCNQ1* gene of patient-derived dermal fibroblasts (HDF) and PSMi006-A cell line (hiPSC). The *KCNQ1* coding sequence (CDS) used as a reference is the NCBI sequence NM_000218.2. **B.** Karyotype analysis of PSMi006-A (300 G-bandings) showing normal female karyotype (46, XX). **C.** PH: phase contrast image showing PSMi006-A morphology. AP: alkaline phosphatase colorimetric staining. The other panels on the right: immunofluorescence stainings showing uniform expression of pluripotency markers in the PSMi006-A. Nuclei were counterstained with Hoechst 33258 (Hoechst, blue). **D.** Immunocytochemistry counting of anti Nanog-positive ($Nanog^+$) and anti TRA-1-60-positive ($TRA\text{-}1\text{-}60^+$) cells. The total number of cells in each of the fields analyzed was quantified by counting the nuclei stained with Hoechst 33258. **E.** RT-PCR analysis showing expression of the indicated markers of pluripotency in PSMi006-A (hiPSC), compared with their parental fibroblasts (HDF). **F.** RT-PCR analysis showing no expression of the four viral transgenes (Tg) in naïve fibroblasts (HDF), expression of Tg OCT4, SOX2, KLF4 and cMYC five days after transduction (OSKM) and silencing of the four Tg in PSMi006-A. **G.** Far left panel: floating embryoid bodies (EBs) formed after 7 days of PSMi006-A culture in suspension. Panels on the right: Immunofluorescence staining for markers of the 3 germ layers in iPSC-derived EBs: neuronal class tubulin beta III (Tuj) for ectoderm, smooth muscle actin (SMA) for mesoderm, and Alpha Fetoprotein (AFP) for endoderm. **H.** Co-immunofluorescence staining for the cardiac sarcomeric proteins alpha-sarcomeric actinin (α-SA, red) and troponin I (TnI, green) in cardiomyocytes differentiated from the PSMi006-A. Nuclei were counterstained with Hoechst. The insets show areas of cross-striations. **I.** EZ-PCR test showing the absence of mycoplasma contamination in PSMi006-A. $Ctrl^+$ is the positive PCR control provided by the kit.

Table 1
Characterization and validation of PSMi006-A cell line.

Classification	Test	Result	Data
Morphology	Photography	Normal	Fig. 1 panel C
Phenotype	Qualitative analysis	Positive immunostaining for the pluripotency markers Oct4, Nanog, Sox2, TRA-1-60, SSEA-3, SSEA-4	Fig. 1 panel C
		Positive staining for the alkaline phosphatase	Fig. 1 panel C
		Expression of the pluripotency markers OCT3/4, SOX2, NANOG, REX1, GDF3, ESG1, DPPA2, DPPA4, NODAL, analyzed by RT-PCR	Fig. 1 panel E
	Quantitative analysis	97,9% $NANOG^+$ cells 91% $TRA\text{-}1\text{-}60^+$ cells	Fig. 1 panel D
Genotype	Karyotype (300 G-banding) and resolution	46XX, Resolution 450–500	Fig. 1 panel B
Identity	Microsatellite PCR (mPCR)	Not performed	Not available
	STR analysis	7 sites tested for iPSC, all sites matched with donor HDF STR profile	Available with the authors
Mutation analysis	Sequencing	Homozygous for the mutation c.535 $G > A$ p.G179S on the KCNQ1 gene	Fig. 1 panel A
Microbiology and virology	Mycoplasma	Mycoplasma testing by RT-PCR. Negative	Fig. 1 panel I
Differentiation potential	Embryoid body formation	The EBs expressed neuronal class tubulin beta III (Tuj) (ectoderm), smooth muscle actin (SMA) (mesoderm), and Alpha Fetoprotein (AFP) (endoderm).	Fig. 1 panel G
	Differentiation into cardiomyocytes	The iPSC-derived cardiomyocytes expressed the cardiac sarcomeric proteins alpha-sarcomeric actinin (α-SA) and troponin I (TnI)	Fig. 1 panel H
Donor screening	HIV 1 + 2 Hepatitis B, Hepatitis C	Not performed	Not available
Genotype additional info	Blood group genotyping	Not performed	Not available
	HLA tissue typing	Not performed	Not available

disease characterized by the prolongation of cardiac repolarization, which is quantified as the duration of the QT interval on the surface electrocardiogram (ECG). This prolonged repolarization time predisposes the patient to develop ventricular arrhythmias that can cause, syncope or sudden cardiac death (SCD) (Schwartz et al., 2012). LQT1 is the commonest LQTS sub-type, accounting for ~40–50% of all cases (Schwartz et al., 2012). It is caused by mutations in the KCNQ1 gene, encoding for the α-subunit of the voltage-dependent potassium channel mediating the I_{Ks} current, which is an important contributor of the action potential (AP) repolarization (Schwartz et al., 2012).

When enrolled, the patient had a markedly prolonged QTc (QT corrected for heart rate) of 576 ms, and she already experienced several episodes of syncope and a documented episode of ventricular fibrillation triggered by emotional stress. Genetic screening revealed the presence of a homozygous c.535 G/A mutation on the KCNQ1 gene, leading to the substitution of the glycine in position 179 with serine. Both her two older sisters carry the same mutation in homozygosis; the firstborn died at age 19 after an intense emotional stress, the second born is still alive but experienced several cardiac episodes (Schwartz, 2012). Finally, her son is heterozygous for the mutation and asymptomatic.

Fibroblasts were reprogrammed by retroviral infection of OCT4, SOX2, KLF4 and c-MYC. The obtained hiPSCs were maintained on feeders, retaining embryonic stem cell (ES)-like morphology (*Fig. 1**C***) and pluripotent features up to passage 50. DNA sequencing proved that both patient's fibroblasts and the derived hiPSCs carry the disease causing mutation on the KCNQ1 gene (*Fig. 1**A**. The KCNQ1 coding sequence -CDS- used as a reference is the NCBI sequence NM_000218.2*), and an identical DNA profile at seven polymorphic loci, as shown by Short tandem Repeat (STR) analysis (available with the authors). Moreover the DNA karyotyping revealed normal female chromosome asset (46, XX) (*Fig. 1**B***). PSMi006-A uniformly expresses the human ES surface antigens Tumor Related Antigen-1-60 (TRA-1-60), Stage Specific Embryonic Antigen-3 and −4 (SSEA-3, SSEA-4) (*Fig. 1**C–D***), and the pluripotent markers NANOG, OCT4, SOX2 (*Fig. 1**C–E***), REX1, GDF3, ESG1, DPPA2, DPPA4 and NODAL (*Fig. 1**E***). Likewise, it shows alkaline phosphatase (AP) activity (*Fig. 1**C***). RT-PCR in *Fig. 1**F*** shows no expression of the four viral transgenes (Tg) in naïve fibroblasts (HDF), clear expression of Tg OCT4, SOX2, KLF4 and cMYC in fibroblasts five days after transduction (OSKM) and silencing of the four Tg in PSMi006-A at passage 5.

PSMi006-A spontaneously forms embryoid bodies (EBs) able to differentiate into cells belonging to the three germ layers: endoderm, mesoderm and ectoderm (*Fig. 1**G***). In addition we successfully differentiated this AR-LQT1 cell line into spontaneously beating cardiac-like cells expressing typical cardiac markers such as the sarcomeric proteins alpha-actinin (α-SA) and troponin I (TnI) (*Fig. 1**H, the insets show areas of cross-striation***). We also excluded the presence of mycoplasma contamination (*Fig. 1**I***).

3. Materials and methods

Expanded protocols are provided as Supplemental Methods.

Table 2
Reagents details.

Antibodies used for immunocytochemistry			
	Antibody	Dilution	Company Cat # and RRID
Pluripotency Markers	Rabbit anti Nanog	1:200	Stemgent *Cat#* 09-0020, *RRID:* AB_2,298,294
	Mouse anti Oct3/4 (C-10)	1:500	SCBT *Cat#* sc-5279, *RRID:* AB_628,051
	Mouse anti Sox2	1:500	R&D Systems *Cat#* MAB2018, *RRID:* AB_358,009
	Mouse anti TRA-1-60	1:100	Stemgent *Cat#* 09-0010, *RRID:* AB_1,512,170
	Rat anti SSEA-3	1:100	Millipore *Cat#* MAB4303, *RRID:* AB_177,628
	Mouse anti SSEA-4	1:100	Stemgent *Cat#* 09-0006, *RRID:* AB_1,512,169
Differentiation Markers (EBs)	Mouse anti neuronal class tubulin beta III (Tuj)	1:500	Covance *Cat#* MMS-435P, *RRID:* AB_2,313,773
	Mouse anti smooth muscle actin	1:1000	Millipore *Cat#* CBL171, *RRID:* AB_2,223,166
	Mouse anti alpha-fetoprotein	1:500	Millipore *Cat#* SCR030, *RRID:* AB_597,591
Cardiac Markers	Rabbit anti Troponin I	1:250	Abcam *Cat#* ab52862, *RRID:* AB_869,983
	Mouse anti alpha actinin	1:800	Sigma Aldrich *Cat#* A7811, *RRID:* AB_476,766
Secondary antibodies	Alexa-Fluor® 488 Goat anti-rabbit IgG	1:500	ThermoFisher Cat# A11008, *RRID*:AB_143,165
	Alexa-Fluor® 488 Goat anti-rat IgM	1:500	ThermoFisher Cat# A21212, *RRID*:AB_11,180,047
	Alexa-Fluor® 488 Goat anti-mouse IgG	1:500	ThermoFisher Cat# A11001, *RRID*: AB_2,534,069
	Alexa-Fluor® 546 Goat anti-mouse IgG	1:500	ThermoFisher Cat# A11003, *RRID*: AB_141,370

Primers		
	Target	Forward/Reverse primer (5′−3′)
Targeted mutation analysis/sequencing	KCNQ1 Exon 3	Fw: 5′- gttcaaacaggttgcagggtctga −3′ Rev: 5′- ccaggtttccagaccaggaag-3′
Pluripotency Markers (RT-PCR)	Oct4	Fw: 5′-gtactcctcggtccctttcc-3′ Rev: 5′-caaaaaccctggcacaaact-3′
	Sox2	Fw: 5′-acaccaatcccatccacact-3′ Rev: 5′-tttttcgtcgcttggagact-3′
	Nanog	Fw: 5′-ttccttcctccatggatctg-3′ Rev: 5′-tctgctggaggctgaggtat-3′
	Rex1	Fw: 5′-cagatcctaaacagctcgcagaat-3′ Rev: 5′-gcgtacgcaaatttaaagtccaga-3′
	GDF3	Fw: 5′-cttatgctacgtaaaggagctggg-3′ Rev: 5′-gtgccaacccaggtcccggaagtt-3′
	ESG1	Fw: 5′-atatcccgccgtgggtgaaagttc-3′ Rev: 5′-actcagccatggactggagcatcc-3′
	DPPA4	Fw: 5′-ggagccgcctgccctggaaaattc-3′ Rev: 5′-tttttcctgatattctattcccat-3′
	DPPA2	Fw: 5′-ccgtccccgcaatctccttccatc-3′ Rev: 5′-atgatgccaacatggctcccggtg-3′
	Nodal	Fw: 5′-gggcaagaggcaccgtcgacatca-3′ Rev:5′-gggactcggtggggctggtaacgtttc-3′
House-Keeping Genes (RT-PCR)	GAPDH	Fw 5′-catgttccaatatgattccaccc-3′ Rev 5′-gggatctcgctcctggaagat-3′
Retroviral transgenes	Oct4 cDNA on pMXs-hOCT3/4	Fw: 5′-ccccagggccccattttggtacc-3′
	Sox2 cDNA on pMXs-hSOX-2	Fw: 5′-ggcacccctggcatggctcttggctc-3′
	cMyc cDNA on pMXs-hcMYC	Fw: 5′-caacaaccgaaaatgcaccagccccag-3′
	Klf4 cDNA on pMXs-hKLF4	Fw: 5′-acgatcgtggccccggaaaaggacc-3′
	pMX viral vector	Rev: 5′-ccctttttctggagactaaataaa-3′

3.1. Generation of hiPSCs

Skin fibroblasts were reprogrammed using four retroviruses encoding OCT4, SOX2, KLF4 and c-MYC. Emerging iPSC clones were manually picked, individually placed into a separate cell culture well and expanded on a feeder-layer of mitotically-inactivated mouse embryonic fibroblasts (iMEF), in DMEM/F12, 20% Knockout Serum Replacement (KO-SR), 2 mM L-glutamine, 50 U/ml penicillin, 50 U/ml streptomycin, 1% Non-Essential Amino Acids (NEAA), 0.1 mM beta-mercaptoethanol, 10 ng/ml basic Fibroblast Growth Factor (bFGF) (*Table 1*).

3.2. Mutation analysis

Genomic DNA from hiPSCs and their parental fibroblasts was amplified with the GoTaq G2 DNA polymerase (Promega) and primers in *Table 2*. The resulting amplicons were purified and sequenced (Lightrun service - GATC Biotech AG – Germany).

3.3. STR analysis

The PowerPlex® CS7 human identification kit (Promega) was used to co-amplify a set of seven variable short tandem repeat loci (LPL, F13B, FESFPS, F13A01, Penta_D, Penta_C, Penta_E) on genomic DNA from fibroblasts and hiPSCs in order to compare the genetic profile of the two cell lines. After PCR-amplification, fragments were run on a 3130xl capillary sequencer (Applied Biosystems) and then analyzed using GeneMarker software (SoftGenetics).

3.4. Karyotyping

hiPSCs were blocked at metaphase by exposure to 10 μg/ml demecolcine solution for 3 h (Sigma Aldrich). Karyotyping was performed using 300 G-banding chromosome analysis.

3.5. Immunocytochemistry

hiPSCs grown on glass coverslips were fixed for 15 min in 4% paraformaldehyde (Affymetrix USB), permeabilized in PBS containing 0.1% Triton X-100 (Sigma Aldrich) for 5 min, and blocked in 1% bovine

serum albumin (BSA, Sigma Aldrich) for 1 h at room temperature (RT). Then they were incubated for 1 h at RT with the primary antibody (*Table 2*) diluted in blocking solution, washed three times, and incubated for 1 h at RT with an appropriate secondary antibody (*Table 2*). Finally, the cells were stained with 1 μg/ml of Hoechst 33,258 (Sigma Aldrich). Images were acquired using the Carl Zeiss fluorescence microscope Observer.Z1 equipped with the Apotome system and AxioVision 6.0 software (Zeiss GmbH, Gottingen, Germany).

3.6. Immunocytochemistry counting

Nanog$^+$ and TRA-1-60$^+$ cells were counted using the AxioVision 6.0 software (Zeiss GmbH, Gottingen, Germany). A total of 1000 cells were counted in 3-4 fields.

3.7. AP colorimetric assay

AP was detected by using the Alkaline Phosphatase Staining kit (00-0009 Stemgent).

3.8. RT-PCR

Total RNA was purified using TRIzol (ThermoFisher Scientific). cDNA was synthesized using the Superscript II Reverse Transcriptase (ThermoFisher). RT-PCR was performed with the GoTaq G2 DNA polymerase (Promega) and primers in *Table 2*.

3.9. EB formation

hiPSCs were enzimatically detached and grown for 7 days in non-adherent conditions in a modified iPS medium deprived of bFGF and containing 20% FBS instead of KO-SR. Forming EBs were then transferred to gelatin-coated dishes to allow differentiation in adhesion in the same medium for additional 7 days. Finally, the cells were processed for immunostaining of the three germ layers as described above.

3.10. Cardiac differentiation

Cardiac differentiation was induced using the PSC Cardiomyocyte Differentiation Kit (ThermoFisher).

3.11. Mycoplasma test

For the detection of mycoplasma in cell culture we used the EZ-PCR Mycoplasma Test Kit (Biological Industries).

Declaration of Competing Interest

None.

Acknowledgements

This work was supported by the Leducq Foundation for Cardiovascular Research [18CVD05] 'Towards Precision Medicine with Human iPSCs for Cardiac Channelopathies', by the Italian Ministry of Health, "Ricerca Corrente" projects numbers 08064017 and 08064018, and by a grant to the Department of Molecular Medicine of the University of Pavia under the initiative "Dipartimenti di Eccellenza" (2018–2022).

Supplementary materials

Supplementary material associated with this article can be found, in the online version, at doi:10.1016/j.scr.2019.101658.

References

Mehta, A., Ramachandra, C.J.A., Singh, P., Chitre, A., Lua, C.H., Mura, M., Crotti, L., Wong, P., Schwartz, P.J., Gnecchi, M., Shim, W., 2018. Identification of a targeted and testable antiarrhythmic therapy for long-QT syndrome type 2 using a patient-specific cellular model. Eur. Heart J. 39, 1446–1455.

Gnecchi, M., Stefanello, M., Mura, M., 2017. Induced pluripotent stem cell technology: toward the future of cardiac arrhythmias. Int. J. Cardiol. 237, 49–52.

Mura, M., Mehta, A., Ramachandra, C.J., Zappatore, R., Pisano, F., Ciuffreda, M.C., Barbaccia, V., Crotti, L., Schwartz, P.J., Shim, W., Gnecchi, M., 2017. The KCNH2-IVS9-28A/G mutation causes aberrant isoform expression and hERG trafficking defect in cardiomyocytes derived from patients affected by long QT syndrome type 2. Int. J. Cardiol. 240, 367–371.

Schwartz, P.J., Crotti, L., Insolia, R., 2012. Long-QT syndrome: from genetics to management. Circ. Arrhythm Electrophysiol. 5, 868–877.

Schwartz, P.J., 2012. The role of the sympathetic nervous system in the long qt syndrome: the long road from pathophysiology to therapy. Card Electrophysiol. Clin. 4, 75–85.